

Ride quality evaluation of the soil compactor cab supplemented by auxiliary hydraulic mounts via simulation and experiment

Nguyen Van Liem^{1,2} Zhang Jianrun¹ Hua Wenlin² Wang Peiling²

(¹School of Mechanical Engineering, Southeast University, Nanjing 211189, China)

(²School of Mechanical and Electrical Engineering, Hubei Polytechnic University, Huangshi 435003, China)

Abstract: In order to evaluate the ride quality of the soil compactor cab supplemented by the auxiliary hydraulic mounts (AHM), a nonlinear dynamic model of the soil compactor interacting with the off-road deformable terrain is established based on Matlab/Simulink software. The power spectral density (PSD) and the weighted root mean square (RMS) of acceleration responses of the vertical driver's seat, the cab's pitch and roll angle are chosen as objective functions in low-frequency range. Experimental investigation is also used to verify the accuracy of the model. The influence of the damping coefficients of the AHM on the cab's ride quality is analyzed, and damping coefficients are then optimized via a genetic algorithm program. The research results show that the cab's rubber mounts added by the AHM clearly improve the ride quality under various operating conditions. Particularly, with the optimal damping coefficients of the front-end mounts $c_{a1,2} = 1\ 500\ \text{N} \cdot \text{s/m}$ and of the rear-end mounts $c_{a3,4} = 2\ 335\ \text{N} \cdot \text{s/m}$, the weighted RMS values of the driver's seat, the cab's pitch and roll angle are reduced by 22.2%, 18.8%, 58.7%, respectively. Under the condition of the vehicle travelling, with the optimal damping coefficients of $c_{a1,2} = 1\ 500\ \text{N} \cdot \text{s/m}$ and $c_{a3,4} = 1\ 882\ \text{N} \cdot \text{s/m}$, the maximum PSD values of the driver's seat, the cab's pitch and roll angle are clearly decreased by 36.7%, 54.7% and 50.6% under the condition of the vehicle working.

Key words: off-road soil compactor; dynamic model; cab's rubber mounts; auxiliary hydraulic mount; ride quality

DOI: 10.3969/j.issn.1003-7985.2019.03.001

The soil compactor often works in the field of the construction site, factories, etc. Its operating principle is a combination of the static force of the vehicle and the dynamic force of the drum to compact the soil ground, asphalt and other materials. The vibration excitations

from the deformable terrain and drum are thus transmitted to the driver through the isolation systems of the cab and the vehicle. Consequently, the cab's isolation system is one of the most important factors to improve the vehicle ride quality.

The basic research of the tire-deformable terrain contact^[1-4] and interaction between the rigid drum and elastic-plastic soil^[5] indicated that the vibration response of the vehicle was greatly influenced by off-road terrains. Almost all the cab's isolation system of soil compactors was equipped by the rubber mounts with high stiffness characteristic and low damping of rubber material^[6-9]. Therefore, the stiff rubber property helped suppress only high-frequency vibrations and noise, contrariwise, the low damping of the natural rubber generated the high magnitude vibrations which can reduce the vehicle's ride quality^[6]. The effects of design parameters of the cab's rubber mounts on the ride quality was evaluated^[7]. An optimal design for the cab's new rubber mounts of soil compactors was built via the finite element model, and the new rubber mount was then produced and tested for the vehicle's cab^[8]. The parameters of the cab's rubber mounts were also optimized to increase the ride quality^[9]. The results showed that the vehicle's ride quality was significantly improved. However, the research results also showed that the large-amplitude shock of the cab existed in the low-frequency region at the direction of forwarding motion. This is one of the reasons that causes the tiredness of the driver while working, cracking surfaces of the cab and other problems. Thus, to solve this problem, the low damping coefficients of the cab's rubber mounts need to be improved.

In this study, a 3-D dynamic model of the soil compactor was established based on the deformable terrain models^[1,4-5]. The vibration excitations consist of the drum/tires-deformable terrain contact under the condition of the vehicle traveling and an excitation (28 Hz) of the drum under the condition of the vehicle working on elastic-plastic soil. Experimental investigation was used to validate the model and verify its accuracy. The cab's rubber mounts were supplemented by auxiliary hydraulic mounts (AHM) to evaluate the ride quality, and the damping coefficients of the AHM were then optimized by the genetic algorithm to enhance the vehicle's ride quality. The per-

Received 2018-09-17, **Revised** 2019-03-10.

Biographies: Nguyen Van Liem (1986—), male, doctor; Zhang Jianrun (corresponding author), male, doctor, professor, zhangjr@seu.edu.cn.

Foundation items: The Science and Technology Support Program of Jiangsu Province (No. BE2014133), the Prospective Joint Research Program of Jiangsu Province (No. BY2014127-01).

Citation: Nguyen Van Liem, Zhang Jianrun, Hua Wenlin, et al. Ride quality evaluation of the soil compactor cab supplemented by auxiliary hydraulic mounts via simulation and experiment[J]. Journal of Southeast University (English Edition), 2019, 35(3): 273–280. DOI: 10.3969/j.issn.1003-7985.2019.03.001.

formance of AHM was evaluated through the weighted RMS and the PSD of acceleration responses of the vertical driver's seat, the cab's pitch and roll angle in the low-frequency region. The aim of this study is to improve the ride quality and control the cab shaking.

1 Soil Compactor Model

1.1 Vehicle dynamic model

A 3-D nonlinear dynamic model of the vehicle with 9 degrees of freedom (DOF) considering the interaction between wheels and off-road terrains is established to evaluate the cab's ride quality (see Fig. 1).

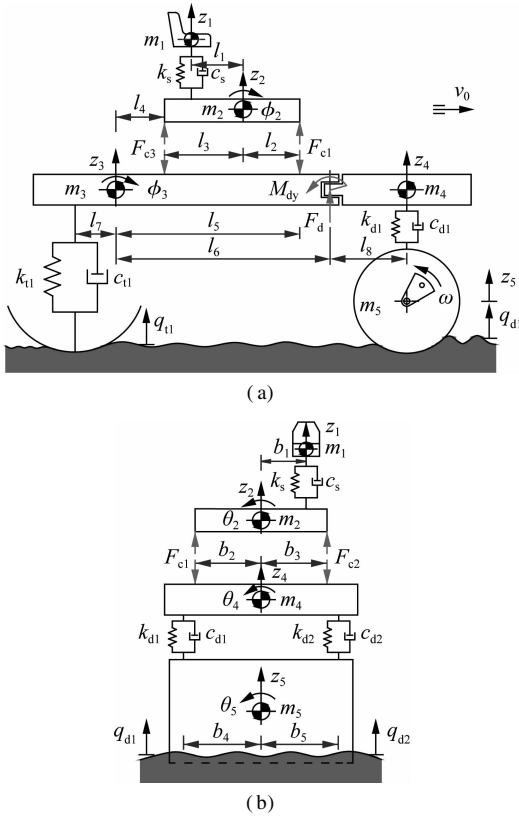


Fig. 1 3-D dynamic model of a vibratory soil compactor. (a) Side view; (b) Front view

As shown in Fig. 1, z_v and m_v are the vertical displacement and mass at the centre of gravity of the driver's seat, the cab, the rear/front vehicle frame and the drum; ϕ_2 and ϕ_3 are the pitch angles at the centre of gravity of the cab and the rear frame; θ_j is the roll angle at the centre of gravity of the cab, the rear/front frame and the drum; k_s , $k_{d1,2}$, $k_{t1,2}$ and c_s , $c_{d1,2}$, $c_{t1,2}$ are the stiffness and damping coefficients of the driver's seat suspension, the drum's rubber mounts and tires, respectively; F_{ci} are the dynamic reaction forces of the cab's isolation mounts; $q_{d1,2}$ and $q_{t1,2}$ are the excitations of the off-road terrains; l_u and b_v are the distances of the vehicle ($i = 1, 2, 3, 4$; $j = 2, 3, 4, 5$; $u = 1, 2, \dots, 8$; $v = 1, 2, \dots, 5$).

Based on the vehicle dynamic model in Fig. 1, and by applying Newton's second law of motion, the motion

equations of the soil compactor can be represented in the matrix form as

$$\mathbf{M}\ddot{\mathbf{Z}} + \mathbf{C}\dot{\mathbf{Z}} + \mathbf{K}\mathbf{Z} = \mathbf{F}(t) \quad (1)$$

where \mathbf{M} , \mathbf{C} and \mathbf{K} are the mass, damping and stiffness matrices, respectively; \mathbf{Z} is the displacement vector; and $\mathbf{F}(t)$ is the exciting force vector.

1.2 Cab's isolation system model

The cab's isolation system of the soil compactor was equipped by four rubber mounts to isolate the transmittal vibration sources from the rear vehicle frame to the cab floor. Due to the low performance of the old rubber mount in improving the ride quality, especially the high pitch angle of the cab, a new optimal design of the cab's rubber mounts was then carried out to improve the cab's ride quality^[8]. However, its vibration isolation performance is still small in the low-frequency region.

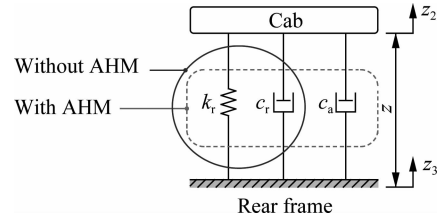


Fig. 2 Cab's isolation system model

In this study, a new rubber mount supplemented by the AHM is proposed to further improve the cab's ride quality. The lumped parameter model is shown in Fig. 2, where k_r and c_r are the stiffness and damping coefficient of the new rubber mount, respectively; c_a is the damping coefficient of the AHM added in the cab's rubber mounts.

The corresponding dynamic force of mount i of the cab's isolation system is given as

$$F_{ci} = \begin{cases} k_{ri}z_i + c_{ri}\dot{z}_i & \text{without AHM} \\ k_{ri}z_i + (c_{ri} + c_{ai})\dot{z}_i & \text{with AHM} \end{cases} \quad (2)$$

where $z_i = z_{2i} - z_{3i}$ and $\dot{z}_i = \dot{z}_{2i} - \dot{z}_{3i}$ are the displacements and the relative velocities of the cab floor and the rear vehicle frame at mount i , and they are given by

$$\begin{aligned} z_{2i} &= z_2 + (-1)^\alpha l_{\alpha+1} \phi_2 + (-1)^i b_\delta \theta_2 \\ z_{3i} &= z_3 - l_v \phi_3 + (-1)^i b_\delta \theta_3 \end{aligned} \quad (3)$$

$$\begin{aligned} \dot{z}_{2i} &= \dot{z}_2 + (-1)^\alpha l_{\alpha+1} \dot{\phi}_2 + (-1)^i b_\delta \dot{\theta}_2 \\ \dot{z}_{3i} &= \dot{z}_3 - l_v \dot{\phi}_3 + (-1)^i b_\delta \dot{\theta}_3 \end{aligned} \quad (4)$$

where $i = 1, 2$, then $\alpha = 1$, $v = 5$ and $\delta = i + 1$; and $i = 3, 4$, then $\alpha = 2$, $v = 4$ and $\delta = i - 1$.

1.3 Vehicle and terrain interaction models

1.3.1 Wheels-deformable soil contact

Under the condition of the vehicle travelling, the drum/tires are assumed to move on a deformable terrain with the terrain surface roughness. Based on the model of

Bakker and Wong^[1-2], when a wheel moves on a random terrain surface $q(t)$ of the deformable terrain, under the effect of the static and dynamic loads of the wheel, the terrain is then sunk by z_{oa} , as shown in Fig. 3. The pressure p_g and the shear stress τ_g arising from the soil compression in the deformable region (arc of oa) thus impact on the wheel. Thus, the reaction force F_g of the terrain under the wheel is given as

$$F_g = \int_0^{\theta(t)} B p_g r \cos \theta d\theta + \int_0^{\theta(t)} B \tau_g r \sin \theta d\theta \quad (5)$$

p_g and τ_g are given by Bakker^[1] as follows:

$$\left. \begin{aligned} p_g &= (k_c/b + k_\varphi) z_x^n \\ \tau_g &= (c + p_g \tan \varphi) (1 - e^{-j/K}) \end{aligned} \right\} \quad (6)$$

where k_c and k_φ are the soil stiffness coefficients for sinkage and internal friction, respectively; n is the sinkage exponent; b is the smaller dimension of the contact patches and the widths of the drum/tire B ; r is the radius of the drum/tire; c is the soil cohesion coefficient; φ is the angle of the internal friction; K is the shear deformation modulus; and $j = rs[\theta_a(t) - \theta]$ in which s is the slip ratio of the drum/tire.

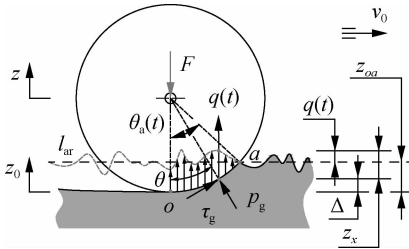


Fig. 3 Wheel-deformable terrain contact model

Assume that l_{ar} is the average roughness line of the terrain surface, and thus, the sinking of the terrain z_x can be determined by $z_x = q(t) + z_{oa} - \Delta$, herein, $q(t)$ is the random excitation of the off-road terrain surface and it is described as follows.

According to the ISO proposal^[10], the spectral density of the off-road terrain surface is written as

$$S(\Omega) = S(\Omega_0) \left(\frac{\Omega}{\Omega_0} \right)^{-w_0}, \quad w_0 = \begin{cases} 3 & \Omega \leq \Omega_0 \\ 0.25 & \Omega > \Omega_0 \end{cases} \quad (7)$$

The value $S(\Omega_0)$ provides a measure for the random terrain with the reference spatial frequency $\Omega_0 = 1/(2\pi)$ cycle/m. More specifically, assuming that the vehicle moves with a constant speed v_0 , the off-road terrain irregularities can then be simulated by

$$q(t) = \sum_{i=1}^N \sqrt{2S(i\Delta n)} \Delta n \sin(i\Delta\omega t + \varphi_i) \quad (8)$$

where N is the number of intervals; φ_i is a random phase uniformly distributed between 0 and 2π ; and $\Delta\omega = \Delta n v_0$ is the fundamental temporal frequency.

The desired terrain roughness can be yielded by choo-

sing a value in the spectral density ranges.

According to the vehicle dynamic model in Fig. 1 and the wheels-deformable soil contact model in Fig. 3, the excitation forces F_t and F_d of the drum and tires are described by

$$\left. \begin{aligned} m_5 \ddot{z}_5 &= F_{dj} - F_{gj} + m_5 g \\ F_{dj} &= k_d(z_4 - z_5) + c_d(\dot{z}_4 - \dot{z}_5) \end{aligned} \right\} \quad j=1,2 \quad (9)$$

$$\left. \begin{aligned} F_{vj} + F_{gj} - m_{tj} g &= 0 \\ F_{vj} &= k_t(z_3 - l_7 \varphi_3 - z_t) + c_t(\dot{z}_3 - l_7 \dot{\varphi}_3 - \dot{z}_t) \end{aligned} \right\} \quad j=1,2 \quad (10)$$

1.3.2 Drum and elastic-plastic soil interaction

The soil compactor uses the most of its time to work on the elastic-plastic soil. Therefore, according to Adam and Kop^[5], a model of the rigid drum and elastic-plastic soil interaction is established in Fig. 4. The elastic-plastic property of soil can be expressed via a plasticity factor ε and a damping ratio of plastic soil γ as

$$\varepsilon = \frac{k_{sp}}{k_{sp} + k_{se}}, \quad \gamma = \frac{c_{se}}{k_{sp}} \quad (11)$$

where ε is the compression ratio; k_{se} is the elastic stiffness; k_{sp} is the compression stiffness; c_{se} is the compression damper.

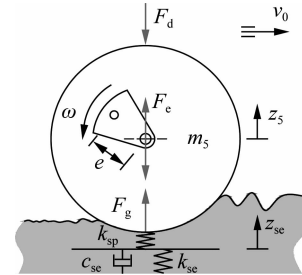


Fig. 4 Rigid drum and elastic-plastic soil interaction model

In a vibration cycle of the drum-soil interaction, there are two or three distinct phases that occur in the motion of the drum and they are described as follows:

1) Loading phase: The gravel-soil ground is compressed by the drum, thus, the density is increased and it has become elastic. The elastic stiffness and compression stiffness of the gravel-soil ground are increased while the compression damper is decreased. In order to describe the relation of z_5 , ε and γ , the vibration equation of the drum is given as^[7]

$$\left. \begin{aligned} \varepsilon \gamma m_5 \ddot{z}_5 + m_5 \ddot{z}_5 &= \varepsilon \gamma F_d + F_d - \varepsilon c_{se} \dot{z}_5 + \dots + \\ &(\varepsilon - 1) k_{sp} z_5 + \varepsilon \gamma m_e \omega^3 \cos \omega t + m_e \omega^2 \sin \omega t \\ F_{dj} &= k_{dj} [z_4 - z_5 + (-1)^j b_{j+3}(\theta_4 - \theta_5)] + \dots + \\ &c_{dj} [\dot{z}_4 - \dot{z}_5 + (-1)^j b_{j+3}(\dot{\theta}_4 - \dot{\theta}_5)] \end{aligned} \right\} \quad (12)$$

2) Unloading phase: The drum moves upward, and the gravel-soil ground is restored. The vibration equation of the drum is written as

$$m_5 \ddot{z}_5 = F_{dj} - c_{se} \dot{z}_5 + m_e \omega^2 \sin \omega t \quad (13)$$

3) Drum-Hope phase: The gravel-soil ground has become elastic, the drum is easy to separate from the soil ground surface, and the vibration equation is written as

$$m_s \ddot{z}_s = F_{dj} + mg + m_e e \omega^2 \sin \omega t \quad j = 1, 2 \quad (14)$$

From Eqs. (12) to (14), the motion of drum z_s and excitation force F_d is then determined.

2 Experimental Model

2.1 Evaluating criteria

The ride quality is mainly evaluated via the weighted RMS acceleration response. In addition, according to ISO 2631-1^[11], the PSD acceleration response are also applied to estimate the effect of vibration on the endurance limit of the human body. It is suggested that a low-frequency range below 10 Hz seriously affected the driver’s health and safety. In this study, the ride quality of the cab’s isolation system is evaluated via the PSD and the weighted RMS of acceleration responses of the vertical driver’s seat, cab’s pitch and roll angle in the frequency and time domains. Thus, the smaller PSD and weighted RMS values mean that the system has the better ability compared to the corresponding isolation mounts. The expression of the weighted RMS value is given as

$$a_{wz} = \sqrt{\frac{1}{T} \int_0^T a_{wt}^2 dt} \quad (15)$$

where a_{wt} is the acceleration (translational and rotational) depending on the duration of the simulation T .

2.2 Experiment model

In order to confirm the model’s accuracy, an experimental condition of the soil compactor using the cab’s new rubber mounts was made under the same simulated condition when the vehicle worked on an elastic-plastic soil ground. Three test steps are described as follows:

Sept 1 Preparation step: Instruments for the experiment include a soil compactor, the Belgium LMS dynamic test and the analysis system; and ICP® three-direction acceleration sensors are used to measure the vibration accelerations. The sensors are installed on the driver’s seat and the cab floor at the four locations of the isolation mounts, as shown in Fig. 5.

Sept 2 Measurement step: The multi-point measurement method is applied, and the process of measurement is performed under an excitation frequency 28 Hz of the drum when the vehicle compacted at a very slow speed $v_0 = 0.83$ m/s.

Sept 3 Data extraction step: The data measurements are carried out including the vertical accelerations at the driver’s seat and at four measurement points on the cab floor.

The acceleration responses of cab’s pitch and roll angle

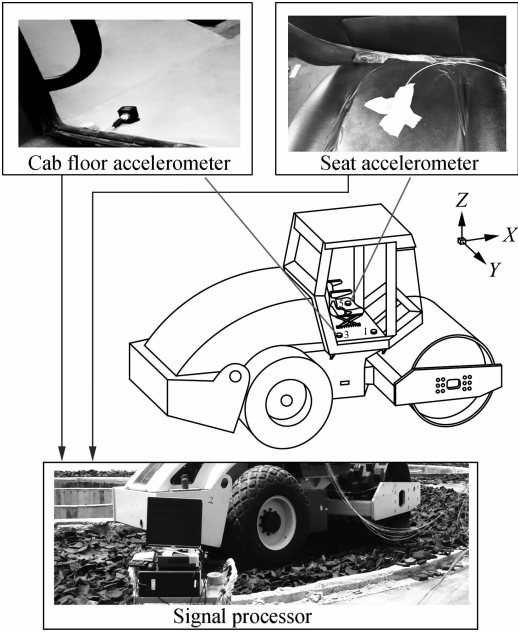


Fig. 5 Diagrammatic sketch of the experimental set-up

are calculated as

$$\ddot{\phi}_c = \frac{\ddot{z}_{c1} - \ddot{z}_{c3}}{l_c}, \quad \ddot{\theta}_c = \frac{\ddot{z}_{c1} - \ddot{z}_{c2}}{b_c} \quad (16)$$

where \ddot{z}_{c1} , \ddot{z}_{c2} , \ddot{z}_{c3} are the vertical accelerations, respectively; l_c and b_c are the distance between measurement points.

Experimental and simulation results of the PSD and weighted RMS of acceleration responses are plotted in Fig. 6 and listed in Tab. 1. The comparison results indicate

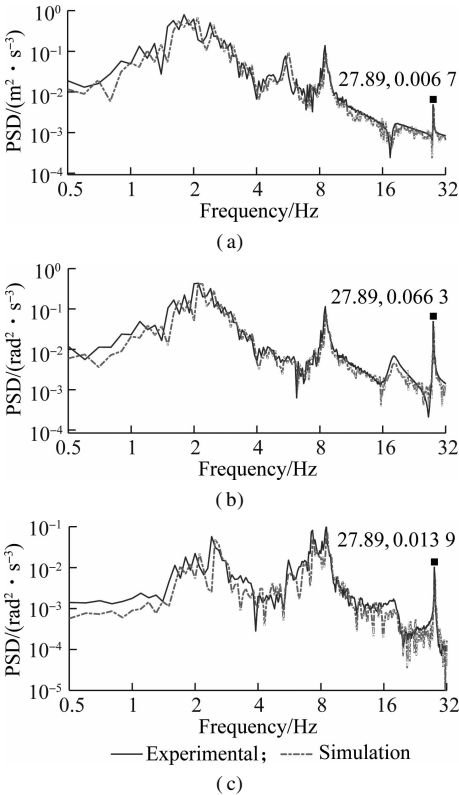


Fig. 6 Acceleration PSD responses of the driver and cab. (a) Driver’s seat heave; (b) Cab pitch angle; (c) Cab roll angle

that the simulation results almost agree with the tests regarding the frequency of the various peaks in the responses and the trend. In addition, the weighted RMS values of the vertical driver's seat, cab's pitch and roll angles also have a small deviation of 10.1%, 11.3% and 12.6% in comparison with the measured values. It implies that the mathematical model of the vibratory roller is an accurate and feasible model.

Tab. 1 Comparison results of experiment and simulation

| Parameter | $a_{wzs}/(m \cdot s^{-2})$ | $a_{w\phi c}/(rad \cdot s^{-2})$ | $a_{w\theta c}/(rad \cdot s^{-2})$ |
|--------------|----------------------------|----------------------------------|------------------------------------|
| Experimental | 0.79 | 0.44 | 0.150 |
| Simulation | 0.71 | 0.39 | 0.131 |
| Deviation/% | 10.1 | 11.3 | 12.6 |

3 Results and Discussion

3.1 Influence of auxiliary hydraulic mounts

3.1.1 Under the condition of the vehicle travelling

In order to evaluate the influence of the damping coefficients of the AHM on the cab's ride quality under the condition of the vehicle traveling, the parameters of the vehicle^[6] and a Grenville soil deformation with its poor terrain classification $q(t)$ ^[3-4] are chosen to simulate at a low vehicle velocity $v_0 = 1.67$ m/s. Assume that the initial damping coefficients of the AHM are $c_0 = 1.5 \times 10^3$ N · s/m. The damping coefficients of AHM $c_{ai} = 0.2c_0, 0.4c_0, \dots, 2.0c_0$ in three different cases of the front-end mounts $c_{a1,2}$, the rear-end mounts $c_{a3,4}$ and all mounts $c_{a1,2,3,4}$ are respectively simulated. The results are shown in Fig. 7.

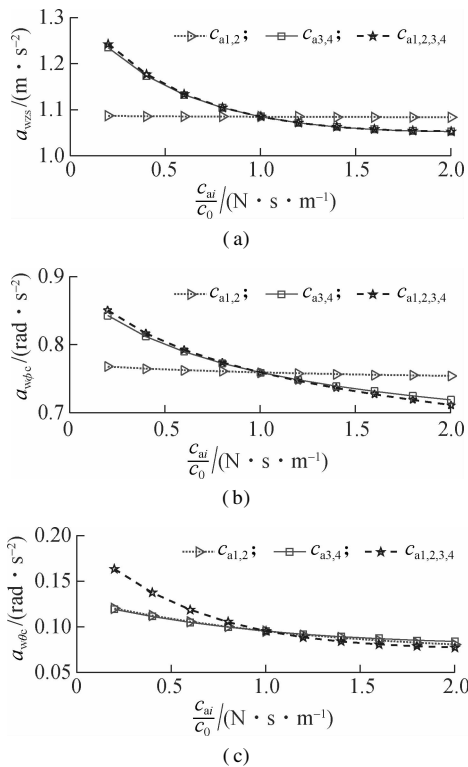


Fig. 7 Effect of the damper coefficients on a soft soil ground. (a) Driver's seat heave; (b) Cab pitch angle; (c) Cab roll angle

Fig. 7 shows that the weighted RMS acceleration responses of the driver's seat heave a_{wzs} , the cab's pitch and roll angle ($a_{w\phi c}$ and $a_{w\theta c}$) are slightly affected by the damping coefficients of the front-end mounts $c_{a1,2}$, whereas these values are strongly affected by the damping coefficients of the rear-end mounts $c_{a3,4}$ and of all mounts $c_{a1,2,3,4}$. However, the influence of $c_{a1,2,3,4}$ on the ride quality is insignificant in comparison with $c_{a3,4}$, thus, $c_{a3,4}$ are chosen to analyze the results. When $0.2c_0 \leq c_{a3,4} \leq 1.6c_0$, the results show that all values of a_{wzs} , $a_{w\phi c}$ and $a_{w\theta c}$ are strongly reduced; when $1.6c_0 \leq c_{a3,4} < 2.0c_0$, all values of a_{wzs} , $a_{w\phi c}$ and $a_{w\theta c}$ are lightly reduced, especially the value of a_{wzs} is tendentially enhanced by $1.8c_0 \leq c_{a3,4} \leq 2.0c_0$, as shown in Fig. 7(a). Thus, the cab's ride quality can be greatly improved when $c_{a1,2} = 1.0c_0$ and $1.2c_0 \leq c_{a3,4} \leq 1.6c_0$.

3.1.2 Under the condition of the vehicle working

Under the condition of the soil compactor working on the workshop, an elastic-plastic soil ground with a high density soil^[5] and a very slow-speed vehicle ($v_0 = 0.68$ m/s) are chosen to simulate under an excitation (28 Hz) of the drum. Also, assume that the initial damping coefficients of AHM are $c_0 = 1.5 \times 10^3$ N · s/m. The damping coefficients $c_{ai} = 0.2c_0, 0.4c_0, \dots, 2.0c_0$ with three different cases of $c_{a1,2}$, $c_{a3,4}$, and $c_{a1,2,3,4}$ are also evaluated, respectively.

The simulation results in Fig. 8 show that the impact of the damping coefficients $c_{a1,2}$, $c_{a3,4}$, and $c_{a1,2,3,4}$ is similar under the condition of the vehicle traveling. Consequently, the damping coefficients of the rear-end mounts, $c_{a3,4}$, are also chosen to analyze the results. Figs. 8(a),

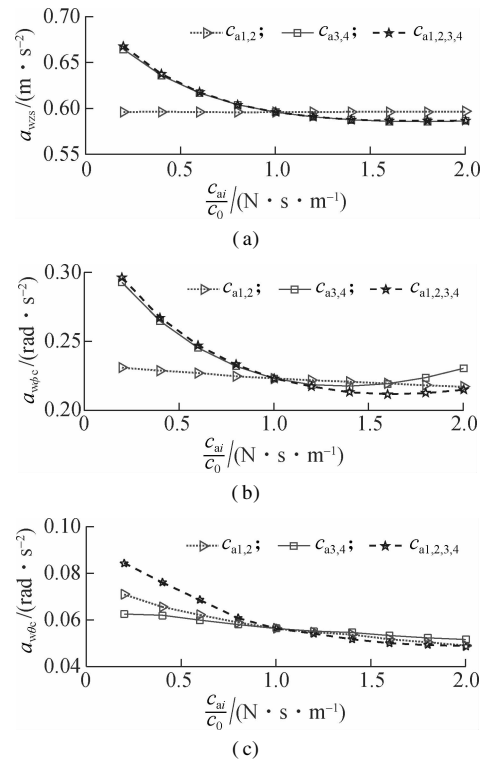


Fig. 8 Effect of the damper coefficients on elastic-plastic soil. (a) Driver's seat heave; (b) Cab pitch angle; (c) Cab roll angle

(b) and (c) show that when $0.2c_0 \leq c_{a3,4} < 1.4c_0$, all the values of a_{wzs} , $a_{w\phi c}$ and $a_{w\theta c}$ are clearly reduced; however, when $1.4c_0 \leq c_{a3,4} \leq 2.0c_0$, the value $a_{w\phi c}$ is significantly enhanced (see Fig. 8(b)). Therefore, the cab's ride quality can be clearly improved when $c_{a1,2} = 1.0c_0$ and $1.0c_0 \leq c_{a3,4} \leq 1.4c_0$.

3.2 Performance of the AHM

The analysis results show that the ride quality is insignificantly affected by $c_{a1,2}$, whereas it is strongly affected by $c_{a3,4}$. The results also show that the ride quality is greatly improved when $1.2c_0 \leq c_{a3,4} \leq 1.6c_0$ under the condition of the vehicle traveling and $1.0c_0 \leq c_{a3,4} \leq 1.4c_0$ under the condition of the vehicle working. In order to choose the optimal values of the damping coefficients, a genetic algorithm program is used to optimize the objective functions.

3.2.1 Genetic algorithm program

The GA is defined as finding a vector variable through constraint conditions to reach the objective function^[12-13], and it is written as

Finding a vector $\mathbf{x} = [x_1, x_2, \dots, x_n]^T$ to optimize

$$F(\mathbf{x}) = [f_1(x), f_2(x), \dots, f_n(x)]^T \quad (17)$$

$$\begin{aligned} \text{s. t.} \quad & g_i(\mathbf{x}) \leq 0 \quad i = 1, 2, \dots, p \\ & h_j(\mathbf{x}) = 0 \quad j = 1, 2, \dots, q \end{aligned}$$

where $F(\mathbf{x})$ is the objective function which must be either maximized or minimized; p and q are the numbers of inequality constraints and equality constraints.

The structure of GA includes encoding, population initialization, fitness evaluation, parent selection, genetic operations and termination criterion.

The goal of the GA is to seek the optimal damping coefficients $c_{a3,4}$ to obtain the minimum a_{wz} values in Eq. (15) via the subsystem model in two cases of the vehicle traveling and working. In order to find the minimum a_{wz} values, the fitness value J is applied to calculate objective functions as^[13-14]

$$J = \frac{1}{\sum \alpha_z a_{wz}^2} \quad (18)$$

s. t.

$$\begin{aligned} \max\{J\} &= \min\{F(\mathbf{x})\} = \min\{a_{wzs}, a_{w\phi c}, a_{w\theta c}\} \\ \mathbf{x} &= [c_{a3}, c_{a4}]^T \end{aligned} \quad (19)$$

where α_z is the weight coefficient of a_{wz} values; $c_{a3,4}$ are the damping coefficients of the AHM at the rear-end mounts, and the initial value of $c_{a3,4}$ for GA under the condition of the vehicle traveling is $1.8 \times 10^3 \leq c_{a3,4} \leq 2.4 \times 10^3$ N · s/m and under the condition of the vehicle working is $1.5 \times 10^3 \leq c_{a3,4} \leq 2.1 \times 10^3$ N · s/m.

The individuals with the higher fitness value J which is obtained via the simulation model show that the obtained damping coefficients $c_{a3,4}$ are good. Therefore, the resultant individuals are updated before the evolution process

ends, and the optimal individuals can be obtained.

In order to seek the optimal values of $c_{a3,4}$ in the cases of the vehicle traveling and working, the weight coefficient α_z respectively are $\alpha_{zs} = 0.548$, $\alpha_{\phi c} = 0.366$ and $\alpha_{\theta c} = 0.086$, which are determined by the percent of a_{wzs} (54.8%), $a_{w\phi c}$ (36.6%) and $a_{w\theta c}$ (8.6%) with the cab's rubber mounts without AHM in Tab. 2. The maximum generation is 600.

Tab. 2 Weighted RMS values on a soft soil ground

| Parameter | $a_{wzs}/(\text{m} \cdot \text{s}^{-2})$ | $a_{w\phi c}/(\text{rad} \cdot \text{s}^{-2})$ | $a_{w\theta c}/(\text{rad} \cdot \text{s}^{-2})$ |
|-------------|--|--|--|
| Without AHM | 1.35 | 0.90 | 0.211 |
| With AHM | 1.05 | 0.73 | 0.087 |
| Reduction/% | 22.2% | 18.8% | 58.7% |

The optimal result in Fig. 9 shows all the fitness values J obtained in the case of the vehicle traveling. The maximum values J are not increased from the evolutionary generation of 462 to the end. Therefore, the optimal individuals can be obtained at the generation of 462, and the optimal value sought via GA is $c_{a3,4} = 2\,335$ N · s/m. Similarly, the optimal value under the condition of the vehicle working is $c_{a3,4} = 1\,882$ N · s/m.

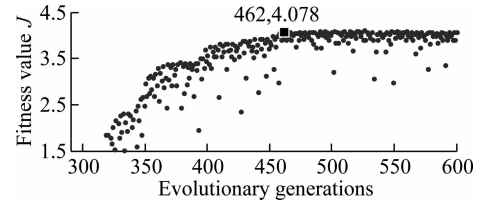


Fig. 9 Fitness results of the optimal running process

3.2.2 Performance on the deformable terrain

With the optimal damping coefficients of $c_{a1,2} = 1\,500$ and $c_{a3,4} = 2\,335$ N · s/m, the weighted RMS and PSD of acceleration responses under the condition of the vehicle travelling are listed in Tab. 2 and shown in Fig. 10. The results in Tab. 2 show that the values of a_{wzs} , $a_{w\phi c}$ and $a_{w\theta c}$ are clearly decreased by 22.2%, 18.8% and 58.7% in comparison with the cab's rubber mounts without AHM.

In addition, the results in Figs. 10(a), (b) and (c) also show that the AHM added in the cab's isolation system have almost no effect on the resonance frequencies of the rubber mounts. In addition, the maximum PSD values of the driver's seat heave, cab's pitch and roll angles are strongly reduced by 35.4%, 33.5% and 48.3% in the low-frequency region (below 10 Hz). Thus, the driver's ride comfort and health are clearly improved by the AHM.

3.2.3 Performance on the elastic-plastic soil

With the optimal damping coefficients of $c_{a1,2} = 1\,500$ and $c_{a3,4} = 1\,882$ N · s/m, the weighted RMS and PSD of acceleration responses under the condition of the vehicle working are also given in Tab. 3 and Fig. 11. The results in Tab. 3 also show that the values of a_{wzs} , $a_{w\phi c}$ and $a_{w\theta c}$ are reduced by 18.3%, 46.1% and 58.8% in comparison with the cab's rubber mounts without AHM.

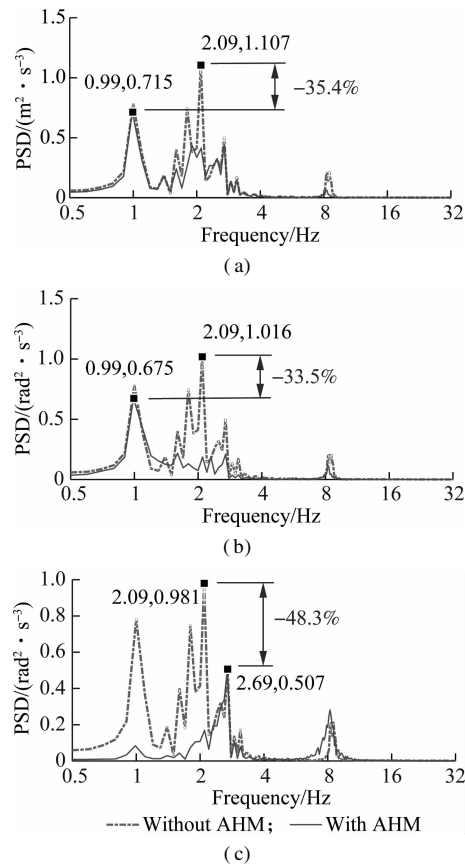


Fig. 10 The acceleration PSD responses on a soft soil ground. (a) Driver's seat heave; (b) Cab pitch angle; (c) Cab roll angle

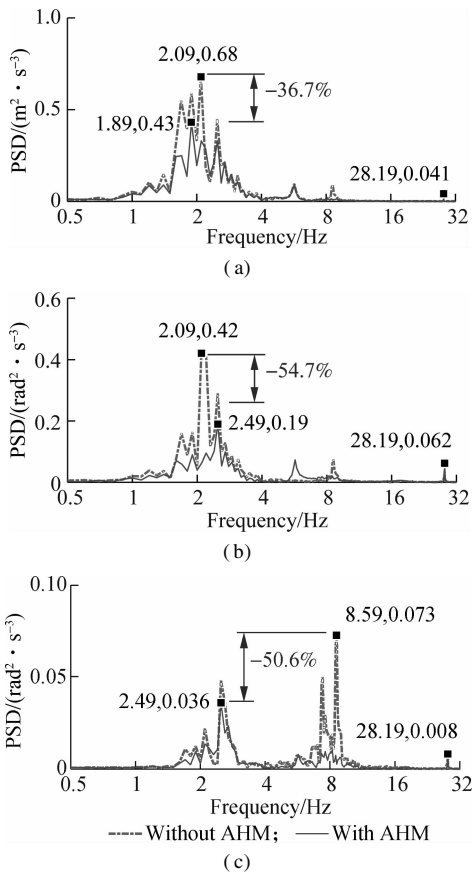


Fig. 11 The acceleration PSD responses on elastic-plastic soil. (a) Driver's seat heave; (b) Cab pitch angle; (c) Cab roll angle

Besides, the results in Figs. 11(a), (b) and (c) also show that the AHM have no effect on the resonance frequencies of the rubber mounts, and the maximum PSD values of the driver's seat heave, cab's pitch and roll angles are clearly decreased by 36.7%, 54.7% and 50.6% in the low-frequency region (below 10 Hz). Consequently, the driver's ride comfort and health are also enhanced by the AHM under the condition of the vehicle working.

Tab. 3 Weighted RMS values on an elastic-plastic soil ground

| Parameter | $a_{wzs}/(m \cdot s^{-2})$ | $a_{w\phi c}/(rad \cdot s^{-2})$ | $a_{w\theta c}/(rad \cdot s^{-2})$ |
|-------------|----------------------------|----------------------------------|------------------------------------|
| Without AHM | 0.71 | 0.39 | 0.131 |
| With AHM | 0.58 | 0.21 | 0.054 |
| Reduction/% | 18.3 | 46.1 | 58.8 |

4 Conclusions

- 1) The driver's ride comfort is strongly affected by the damping coefficients $c_{a3,4}$ of the AHM under the operation conditions of the vehicle.
- 2) With optimal damping coefficients $c_{a1,2} = 1\,500$ and $c_{a3,4} = 2\,335\, N \cdot s/m$, the weighted RMS acceleration responses of the driver's seat, the cab's pitch and roll angle are clearly reduced by 22.2%, 18.8%, 58.7% under the condition of the vehicle travelling.
- 3) With optimal damping coefficients $c_{a1,2} = 1\,500$ and $c_{a3,4} = 1\,882\, N \cdot s/m$, the maximum PSD acceleration responses of the driver's seat, the cab's pitch and roll angle are greatly decreased by 36.7%, 54.7% and 50.6% under the condition of the vehicle working. Therefore, the vehicle's ride quality is significantly improved by auxiliary hydraulic mounts.

References

[1] Bekker M. *Introduction to terrain-vehicle systems*[M]. Ann Arbor, USA: University of Michigan Press, 1969.

[2] Wong J. *Theory of ground vehicles*[M]. New York, NY, USA: John Wiley & Sons, 2001.

[3] Mitschke M. *Dynamik der Kraftfahrzeuge*[M]. Berlin: Springer-Verlag, 1972. DOI: 10.1007/978-3-662-11585-5.

[4] Nguyen V L, Zhang J R, Jiao R Q et al. Effect of the off-road terrains on the ride comfort of construction vehicles[J]. *Journal of Southeast University (English Edition)*, 2019, **35**(2): 191 – 197. DOI: 10.3969/j.issn.1003 – 7985.2019.02.008.

[5] Adam D, Kopf F. Theoretical analysis of dynamically loaded soils [C]//*Proceedings of European Workshop Compaction of Soils and Granular Materials*. Paris, France, 2000: 207 – 220.

[6] Nguyen V L, Zhang J R, Le V Q, et al. Vibration analysis and modeling of an off-road vibratory roller equipped with three different cab's isolation mounts [J]. *Shock and Vibration*, 2018, **2018**: 8527574-1-8527574-17. DOI: 10.1155/2018/8527574.

[7] Kordestani A, Rakheja S, Marcotte P, et al. Analysis of ride vibration environment of soil compactors[J]. *SAE In-*

ternational Journal of Commercial Vehicles, 2010, **3**(1): 259 – 272. DOI: 10.4271/2010-01-2022.

[8] Li J Q, Zhang Z F, Xu H G, et al. Dynamic characteristics of the vibratory roller test-bed vibration isolation system: Simulation and experiment[J]. *Journal of Terramechanics*, 2014, **56**: 139 – 156. DOI: 10.1016/j.jterra.2014.10.002.

[9] Le V Q, Nguyen K T. Optimal design parameters of cab’s isolation system for vibratory roller using a multi-objective genetic algorithm[J]. *Applied Mechanics and Materials*, 2018, **875**: 105 – 112. DOI: 10.4028/www.scientific.net/amm.875.105.

[10] International Organization for Standardization. ISO/TC108/SC2/WG4 N57 Reporting vehicle road surface irregularities [S]. Stuttgart, Germany: Thieme Medical Publishers, 1982.

[11] International Organization for Standardization. ISO 2631 – 1 Mechanical vibration and shock—Evaluation of human exposure to whole body vibration—Part 2: General requirement [S]. Geneva, Switzerland: International Organization for Standardization, 1997.

[12] Nariman-Zadeh N, Salehpour M, Jamali A, et al. Pareto optimization of a five-degree of freedom vehicle vibration model using a multi-objective uniform-diversity genetic algorithm (MUGA)[J]. *Engineering Applications of Artificial Intelligence*, 2010, **23**(4): 543 – 551. DOI: 10.1016/j.engappai.2009.08.008.

[13] Crews J H, Mattson M G, Buckner G D. Multi-objective control optimization for semi-active vehicle suspensions [J]. *Journal of Sound and Vibration*, 2011, **330**(23): 5502 – 5516. DOI: 10.1016/j.jsv.2011.05.036.

[14] Wang W, Song Y L, Xue Y B, et al. An optimal vibration control strategy for a vehicle’s active suspension based on improved cultural algorithm[J]. *Applied Soft Computing*, 2015, **28**: 167 – 174. DOI: 10.1016/j.asoc.2014.11.047.

基于振动压路机驾驶室辅助液阻隔振的平顺性仿真与实验

阮文廉^{1,2} 张建润¹ 华文林² 王培玲²

(¹东南大学机械工程学院, 南京 211189)
(²湖北理工学院机电工程学院, 黄石 435003)

摘要:为了评价振动压路机驾驶室辅助液力的平顺性,基于 Matlab/Simulink 软件建立了振动压路机与变形土壤地面相互作用的非线性动力学模型.以加速度加权均方根值(RMS)和加速度功率谱密度(PSD)响应为目标函数,对不同工况下驾驶员座椅垂向低频振动,驾驶室的俯仰和倾斜低频晃动进行了仿真分析.同时进行了试验以验证模型的准确性.分析了辅助液压隔振的阻尼参数对驾驶室乘坐舒适性的影响,并通过遗传算法对阻尼系数进行优化.研究表明,在不同工况条件下,驾驶室橡胶隔振辅助液压隔振对振动压路机的舒适性均有较大的改善.特别地,在车辆行驶条件下,辅助液压隔振的优化阻尼系数为 $c_{al,2} = 1\,500\text{ N}\cdot\text{s/m}$ 和 $c_{a3,4} = 2\,335\text{ N}\cdot\text{s/m}$;驾驶室座椅垂向振动,驾驶室的俯仰和倾斜晃动的加速度加权均方根值分别降低了 22.2%, 18.8% 和 58.7%;在车辆工作条件下,辅助液压隔振的优化阻尼系数为 $c_{al,2} = 1\,500\text{ N}\cdot\text{s/m}$ 和 $c_{a3,4} = 1\,882\text{ N}\cdot\text{s/m}$;驾驶室座椅垂向振动,驾驶室的俯仰和倾斜晃动的最大 PSD 值分别降低了 36.7%, 54.7% 和 50.6%.

关键词:振动压力机;动力学模型;驾驶室橡胶隔振;辅助液压隔振;平顺性

中图分类号:U461.3